

# Body doubles: an integrative taxonomic approach reveals new sibling species of land planarians

Silvana Vargas do Amaral<sup>A,B</sup>, Giovana Gamino Ribeiro<sup>C</sup>, Victor Hugo Valiati<sup>B,C</sup>  
and Ana Maria Leal-Zanchet<sup>A,B,D</sup>

<sup>A</sup>Instituto de Pesquisas de Planárias, Universidade do Vale do Rio dos Sinos – UNISINOS, São Leopoldo, Brazil.

<sup>B</sup>Programa de Pós-Graduação em Biologia, Universidade do Vale do Rio dos Sinos – UNISINOS, São Leopoldo, Brazil.

<sup>C</sup>Laboratório de Biologia Molecular, Universidade do Vale do Rio dos Sinos – UNISINOS, São Leopoldo, Brazil.

<sup>D</sup>Corresponding author. Email: [zanchet@unisin.br](mailto:zanchet@unisin.br)

**Abstract.** Records of cryptic species have continued to emerge in the scientific literature, often revealed by the use of molecular phylogenetic analyses in an integrative taxonomic approach. This study addresses a group of four striped flatworms from the genus *Pasipha* Ogren & Kawakatsu, showing a pale median stripe on a dark dorsal surface. Based on morphological and molecular analyses from the cytochrome *c* oxidase subunit I gene (*COI*), we establish that we are dealing with sibling species that are closely related to *P. brevilineata* Leal-Zanchet, Rossi & Alvarenga, 2012, a recently described species with a similar colour pattern. Thus, we describe three of the studied flatworms as new species and propose one new unconfirmed candidate species based on molecular data. In addition, sequence analysis revealed 40 nucleotide autapomorphies supporting the species studied herein. Considering anatomical and histological features, the three new species are differentiated from their congeners mainly by details of the copulatory apparatus, such as the occurrence of an epithelium of pseudostratified appearance lining the female atrium and the shape and position of the proximal portion of the prostatic vesicle.

**Additional keywords:** DNA barcoding, cryptic species, Geoplaninae, integrative taxonomy, land flatworms, phylogeny.

Received 26 April 2017, accepted 13 September 2017, published online 4 May 2018

## Introduction

Records of cryptic species are emerging, often revealed by studies on DNA variation (Saez and Lozano 2005; Bickford *et al.* 2007). Usually, two or more species are considered to be cryptic species if they are, at least superficially, morphologically indistinguishable, so that they have been classified as a single nominal species. Cryptic species have been regarded by many authors to be synonymous with sibling species, whereas others specify that sibling connotes more recent common ancestry than does the word cryptic, thus indicating a sister-species relationship (Saez and Lozano 2005; Bickford *et al.* 2007). There may be difficulties in distinguishing between such species, but often some key morphological characters may be found for their identification after detailed comparisons of morphological and non-morphological features. In such cases, we can then refer to pseudo-cryptic or pseudo-sibling species (Saez and Lozano 2005). Excessively broad species delineations may result from the use of mainly morphological characters with insufficient power of resolution to delimit cryptic species. The inclusion of molecular phylogenetic analyses in taxonomic studies may be useful to reveal many genetically distinct lineages in one apparently morphologically uniform unit, thus helping

to differentiate species (Frankham *et al.* 2012; Álvarez-Presas *et al.* 2015).

In land planarians, species identification is based mainly on the morphology of the reproductive system, combined with external features, such as colour pattern and eye arrangement, as well as body musculature and pharyngeal anatomy (Winsor 1998; Seitenfus and Leal-Zanchet 2004). More rarely, some ecological aspects may help to distinguish between species (Álvarez-Presas *et al.* 2015). Thus, application of molecular phylogenetic analyses in taxonomic studies is very useful to uncover specific differences that are not clearly evident on a morphological level. In addition, these analyses may help to identify species from immature specimens, which lack a copulatory apparatus (Álvarez-Presas *et al.* 2015; Carbayo *et al.* 2016; Sluys *et al.* 2016).

Recently, land flatworms with a characteristic striped pattern have been collected from different human-disturbed areas, as well as from a private reserve, in south Brazil. Morphological analyses revealed that they belong to the genus *Pasipha* Ogren & Kawakatsu, 1990. These flatworms show a more-or-less evident, pale median stripe on a homogeneous brownish dorsal surface, with some variations, suggesting that they may constitute

a species complex. The same colour pattern also occurs in *Pasipha brevilineata* Leal-Zanchet, Rossi & Alvarenga, 2012, a species recently described from southern Brazil (Leal-Zanchet *et al.* 2012).

In some species of *Pasipha*, which are anatomically similar, colour pattern and eye arrangement have been useful for differentiation between species (Leal-Zanchet *et al.* 2012; Amaral and Leal-Zanchet 2016; Negrete and Brusa 2016). However, besides the similar colour pattern, the striped flatworms that are herein studied also show similar eye arrangement along the body. Thus, in order to investigate whether external features, as well as anatomical characters of the copulatory apparatus, represent intra- or interspecific variations within this species complex, we use molecular data based on DNA barcoding combined with anatomical information. In addition, we investigate the occurrence of molecular autapomorphies in the flatworms constituting this species complex, as well as in the type species of the genus, *Pasipha pasipha* (Marcus, 1951).

## Material and methods

Land flatworms were collected during the day and night in human-disturbed habitats located in the neighbourhood of remnants of semi-deciduous and deciduous forest in the state of Rio Grande do Sul, and mixed ombrophilous forest in the state of Paraná, south Brazil. Sampling was done by hand in leaf litter and under fallen logs and stones.

Colour pattern and body shape and dimensions were analysed in live specimens. Subsequently, the posterior tip of specimens was amputated and preserved in 100% ethyl alcohol for molecular analysis (Supplementary Material Table S1). Specimens were then euthanised with boiling water. After that, they were immediately fixed in neutral 10% formalin and posteriorly stored in 70% ethyl alcohol. For histological processing of the material and analysis of external and internal characters, methods described by Rossi *et al.* (2015) were used. Histological sections were done at intervals of 6 µm and stained with Goldner's Masson or haematoxyline/eosine.

Type specimens and other individuals that were examined are deposited in the Museu de Zoologia da Universidade do Vale do Rio dos Sinos, São Leopoldo, Rio Grande do Sul, Brazil (MZU), and the Helminthological Collection of Museu de Zoologia da Universidade de São Paulo, São Paulo, state of São Paulo, Brazil (MZUSP). The specimens collected and locality data are listed in Table S1 and in their respective sections of the taxonomic account presented below.

Immature specimens indicated as independent entities by the molecular analyses were treated as unconfirmed candidate species (UCS), following the nomenclature of Vieites *et al.* (2009).

## Molecular analyses

### DNA extraction, PCR amplification and DNA sequencing

Whole-genomic DNA from 41 specimens of *Pasipha* was extracted (Table S1) using the Wizard Genomic DNA Purification Kit (Promega, Madison, WI, USA) according to the manufacturer's instructions. The following primers were used for amplification of a fragment of ~800 base pairs (bp) of

cytochrome *c* oxidase subunit I gene (*COI* gene): BarT (5'-ATG ACD GCS CAT GGT TTA ATA ATG AT-3') (Álvarez-Presas *et al.* 2011); COIR (5'-CCW GTY ARM CCH CCW AYA GTA AA-3') (Lázaro *et al.* 2009) in a 25 µL reaction volume containing 20–50 ng of genomic DNA, 0.2 µM of each primer, 200 µM deoxynucleotides, 1× buffer, 1.5 mM MgCl<sub>2</sub>, 1 unit of *Taq* DNA polymerase (Invitrogen, Carlsbad, CA, USA) and ultrapure H<sub>2</sub>O. The PCR cycling conditions were generated by an initial denaturation step of 3 min at 95°C, followed by 35 cycles of denaturation at 94°C for 50 s, annealing at 50°C for 60 s and extension at 72°C for 50 s, with an additional final extension of 72°C for 5 s. For checking PCR results, agarose gel electrophoresis in 1% agarose gels stained with GelRed (Biotium, Hayward, CA, USA) was used and visualised under UV transillumination. PCR products were purified using Shrimp Alkaline Phosphatase (SAP) and exonuclease I (New England Biolabs, Ipswich, MA, USA), following the manufacturer protocols. Amplicons were direct sequenced at Macrogen (Macrogen Inc., Seoul, Korea), each sample in both directions.

### Molecular data, phylogenetic reconstruction and species delimitation analyses

ChromasPro software (<http://www.technelysium.com.au>) was used to evaluate the quality of sequencing by verifying the chromatogram. Sequences were automatically aligned (with minor manual correction) in ClustalW and MEGA 6 (Tamura *et al.* 2013), with later edition in BioEdit 5.0.9 (Hall 1999). A consensus sequence was generated based on the alignment of two independent sequences. The BLASTn online tool was also used to check the sequences in order to compare with sequences deposited in the GenBank database (NCBI). The amino acid translation was examined to ensure that no gaps or stop codons were present in the alignment. The sequences used herein are publicly available in GenBank (Table S1).

SeaView 4 (Guindon and Gascuel 2010) was used to perform Maximum likelihood (ML) analysis and MrBayes 3.2 (Ronquist *et al.* 2012) was used for Bayesian analysis. jModelTest 2.1.4 (Darriba *et al.* 2012) was used to estimate the evolutionary model that best fits the nucleotide dataset, which was generalised time reversible + gamma + proportion of invariable sites (GTR + G + I), with  $-\ln L = 4044.7671$ ,  $G = 1.0743$  and  $I = 0.5156$  according to the Akaike Information Criterion (AIC; Akaike 1974). The ML tree was constructed using a heuristic search to find the most probable topologies based on the substitution models; statistical support was determined using 1000 bootstrap pseudoreplicates (Felsenstein 1985). Markov chain Monte Carlo was run for  $5 \times 10^6$  generations with two parallel runs, each with four simultaneous chains, sampling every 1000 generations. In order to ensure that the average split frequencies between the runs was less than 1%, the first 25% trees were discarded as a burn-in, after which the chain reached stationarity. Nodes with bootstrap values >70 (ML) and Bayesian posterior probabilities (BI) >0.95 were considered to be significant. MEGA 6 (Tamura *et al.* 2013) was used to calculate pairwise nucleotide distances between all sequences according to Kimura-2-parameter model (K2P) and 1000 bootstraps (Kimura 1980). In addition, the dataset was analysed in PAUP\*4.0b10 (Swofford 2002) in order to verify molecular autapomorphies and calculate the consistency index of each character using heuristic

parsimony analysis, with 100 random stepwise additions of taxa (tree bisection–reconnection branch swapping) under ACCTRAN and DELTRAN optimisation. After the log-file option was activated, sequence data were then used to obtain a labelled tree with a complete list of apomorphies (Describetrees/root = outgroup plot = phylogram labelnode = yes apolist = yes).

#### OTU delineation based on DNA barcodes

Molecular operational taxonomic units (MOTUs) have frequently been used to infer putative species limits. Species boundaries were estimated using three bioinformatic tools: (1) the automatic barcode gap discovery tool (ABGD) (Puillandre *et al.* 2012); (2) coalescent tree-based methods (the generalised mixed Yule-coalescent model (GMYC); Fujisawa and Barraclough 2013); and (3) the Poisson Tree Processes (PTP) model (Zhang *et al.* 2013). ABGD has been used to detect the breaks in the distribution of genetic pairwise distances, referred to as the ‘barcode gap’ (Hebert *et al.* 2003), based entirely on genetic distance between DNA sequences. In addition, GMYC, which is a model-based likelihood method, has been generally considered an effective method to detect species boundaries (Lelièvre *et al.* 2009). It determines the transition signal from speciation to coalescent branching patterns based on a pre-existing ultrametric tree. In order to infer putative species boundaries using the Poisson Tree Processes (PTP) model approach, based on our inferred molecular phylogeny, the maximum likelihood using RAxML (Stamatakis 2006) was employed as input data to PTP.

The ABGD method was implemented based on all available *COI* sequences and using the online version of the program (<http://www.wabi.snv.jussieu.fr/public/abgd/>), with default value of relative gap width ( $X = 1.0$ ) and K2P (Kimura 1980) as the model of nucleotide evolution. The single-threshold GMYC method was implemented in the R package ‘splits’ (SPecies Limits by Threshold Statistics) (Monaghan *et al.* 2009), using the ultrametric tree based on *COI* gene produced by BEAST v.2.2.1 (Bouckaert *et al.* 2014) and nucleotide substitution models (GTR + G + I) determined by jModelTest. Six independent runs were performed using the following parameters: length of the Markov chain settled to  $1 \times 10^8$  generations; trees and parameters sampled every 1000 generations. The LogCombiner was used to combine the multiple independent runs of BEAST, TreeAnnotator to summarise the information from these trees and Tracer to check the convergence of the runs. The calculations for PTP were conducted on the bPTP webserver (<http://species.h-its.org/ptp/>), with default settings. The corresponding analyses were carried out using trees with the maximum likelihood solution from the ML analyses and the majority-rule consensus topology resulting from the BI analyses.

#### Abbreviations used in the figures

The following abbreviations are used in the figures.

cm, cutaneous musculature; cmc, common muscle coat; cg, cyanophil glands; cov, common glandular ovovitelline duct; cs: creeping sole; db, dorsal band; de, dorsal epidermis; df, dorsal fold; di, dorsal insertion of pharynx; dm, dorsal cutaneous musculature; dsm, dorsal subcutaneous muscles; e, eyes; eg, erythrophil secretion; ej, ejaculatory duct; es, oesophagus; fa, female atrium; fc, female canal; fpv, forked portion of prostatic

vesicle; gm, glandular margin; go, gonoduct; i, intestine; im, internal musculature of pharynx; ls, lateral stripe; lu, pharyngeal lumen; ma1, ental region of male atrium; ma2, ectal region of male atrium; mm, mesenchymal musculature; me, monolobate eyes; mo, mouth; ms, median stripe; n, nerve cord; o, ovary; om, outer musculature of pharynx; ov, ovovitelline duct; pp, pharyngeal pouch; ps, paramedian stripes; pv, prostatic vesicle; sbm, sub-intestinal transversal muscles; sc, secretory cells; sd, sperm duct; sg, shell glands; sp, sensory pit; sv, spermiducal vesicle; spm, supra intestinal transversal muscles; t, testes; te, trilobate eyes; upv, unforked portion of prostatic vesicle; v, vitellaria; ve, ventral epidermis; vi, ventral insertion of pharynx; vm, ventral cutaneous musculature; xg, xanthophil glands.

## Results

### Molecular results

A strongly supported monophyletic group of *Pasipha* (bootstrap = 96%;  $P = 1$ ) including the clades with four operational taxonomic units (MOTUs), besides *Pasipha brevilineata*, was recovered by Bayesian and ML analyses. The MOTUs correspond to three new species and one unconfirmed candidate species *sensu* Vieites *et al.* (2009) for the genus (Figs 1, 2A). *Pasipha variistriata* Amaral & Leal-Zanchet, sp. nov. was indicated as the most basal species in the clade containing the four species herein studied. The monophyly of these four species (bootstrap >90%; pp. >0.95) was also strongly supported by the molecular phylogenetic analyses, which indicated *P. brevilineata* as the sister-species of the group of species herein studied.

A total of 232 bp (29.7%) variable nucleotide sites was detected in the *COI* gene (out of a total of 750 bp nucleotide sites and 54 specimens included in the analyses). No insertions, deletions, NUMTs (nuclear DNA sequences originating from mitochondrial DNA sequences) or stop codons were identified in any sequence. All amplified sequences correspond to functional mitochondrial genes as indicated by the absence of stop codons. The mean interspecific K2P distance for all specimens of *Pasipha* was 9.3%, ranging from 4.5% (*Pasipha albicaudata* Amaral & Leal-Zanchet, sp. nov.  $\times$  *Pasipha brevilineata*) to 12.7% (*Pasipha pasipha*  $\times$  *Pasipha brevilineata*). The intraspecific variation ranged from 0% to 0.5% with the exception of the two specimens of *Pasipha chimbeva* (Froehlich, 1954) (5.4%). Unexpected intraspecific distances were also observed in two specimens of *Imbira marcusii* Carbayo *et al.*, 2013 (5.0%), which were included as the outgroup.

The well supported monophyletic haplogroup formed by the four species herein studied, besides *P. brevilineata*, shares 145 molecular synapomorphies, as revealed by the maximum-parsimony analysis in a segment of the *COI* gene of 530 bp used as the dataset. Molecular transformations were optimised on a strict consensus (481 steps; consistency index (CI) 0.659). Moreover, 40 molecular autapomorphies were inferred for the species herein studied, distributed as follows: 15 (*Pasipha albicaudata*); 12 (*Pasipha variistriata*); 7 (*Pasipha* sp.) and 6 (*Pasipha paucilineata* Amaral & Leal-Zanchet, sp. nov.) (Fig. S1; Table S2).

The results of the ABGD method showed a multimodal pairwise genetic distance (K2P) distribution with a barcode

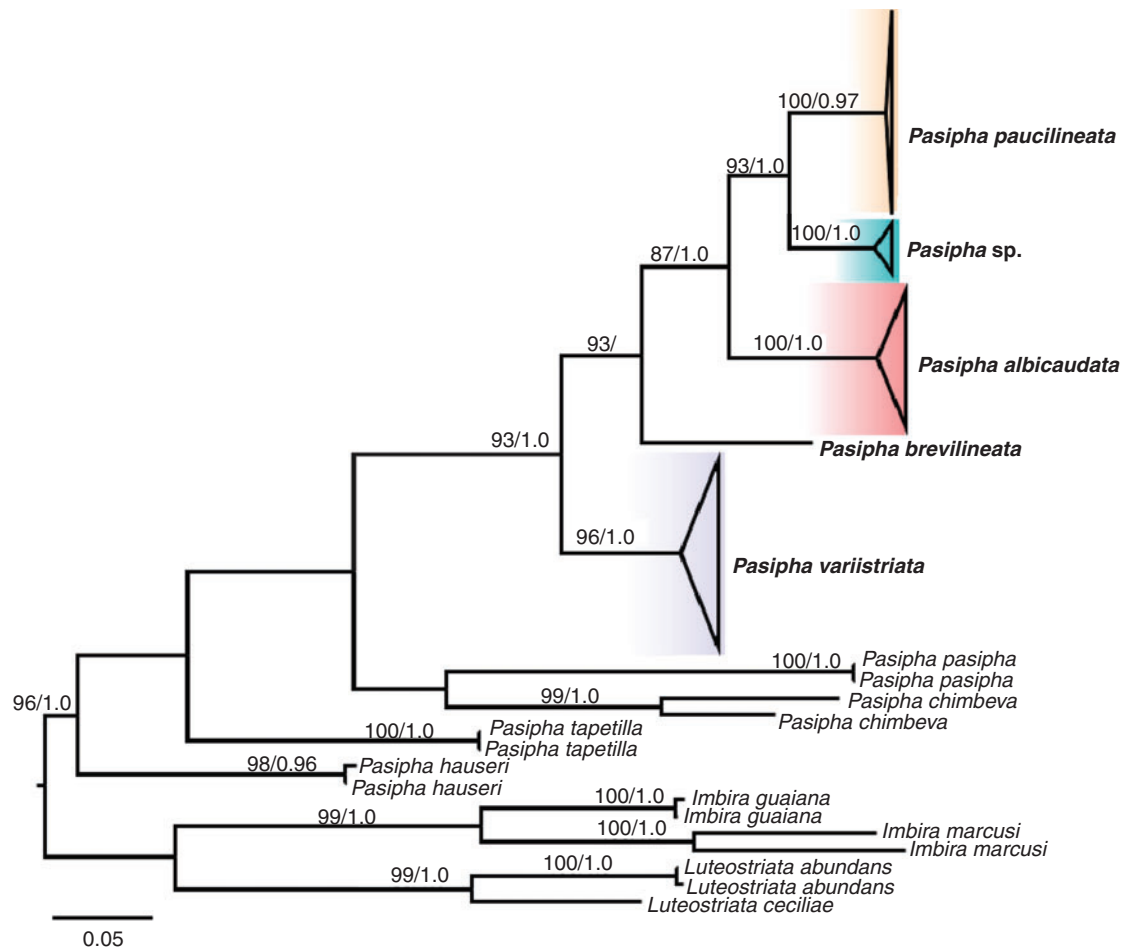


**Fig. 1.** Maximum likelihood phylogenetic tree inferred from the 750 bp of cytochrome *c* oxidase subunit I gene under model selected generalised time reversible (GTR) + gamma distribution shape parameter ( $G = 1.0743$  + proportion of invariable sites ( $I = 0.5156$ ) + G model of sequence evolution. The colours highlight the clades with the four studied species. Values indicate support for each node according to the bootstrap support values >70 and maximum posterior probabilities >0.95, respectively. Scale bar: number of changes per site.

gap located in the range of 1.2–3% distance, detecting 15 molecularly defined MOTUs with estimated prior maximum divergence of intraspecific diversity (P) of 2% (Fig. 2B). Likewise, ABGD analysis identified both specimens of *Pasipha chimbeva*, as well as both specimens of *Imbira marcusi* as independent entities. Species delimitation analyses performed by implementing the coalescent tree-based approach (GMYC model), using an ultrametric phylogenetic tree created in BEAST, exhibited a significantly better likelihood than the null model ( $P < 0.001$ ;  $\log L_{\text{GMYC}} = 357.0519$ ,  $\log L_{\text{NULL}} = 340.6769$ ), thus indicating that a limit between and within species was achieved. Fifteen maximum likelihood entities were identified, of which four corresponded to the specimens used in this study (Fig. 2C). PTP analyses, based on the best-fit ML (Fig. S2), recognised 15 species from a dataset of 54 specimens (Fig. 2D), congruent with the number of putative species recovered by the GMYC and ABGD approaches.

In conclusion, results of species delimitation analyses clearly distinguish four taxa, three of which are herein formally described as new species. The remaining entity (*Pasipha* sp.) is considered

an unconfirmed candidate species. Their specimens are immature and, thus, a full morphological description cannot be given.

## Taxonomy

Family **GEOPLANIDAE** Stimpson

Subfamily **GEOPLANINAE** Stimpson

Genus ***Pasipha*** Ogren & Kawakatsu

***Pasipha albicaudata*** Amaral & Leal-Zanchet, sp. nov.

<http://zoobank.org/urn:lsid:zoobank.org:act:9A3EECBE-6939-4607-846D-5A02776C1526>

## Material examined

*Holotype*. MZUSP PL. 2096; coll. A. M. Leal-Zanchet, 30.x.2013, Salvador do Sul (29°26'26"S, 51°30'28"W), Rio Grande do Sul (RS), Brazil – anterior tip; transverse sections on 14 slides; anterior region at the level of the ovaries:



Dorsal surface of live animals light brown, with a pale yellow median stripe and irregular, dark brown lateral stripes (Fig. 3A). Some specimens with dorsal surface dark-brown and median stripe visible only on posterior tip (Fig. 3B). After fixation, dorsal colour dark brown; thin median stripe bordered by dark brown to black paramedian stripes (Fig. 3C). Ventral surface pale grey or pale yellow, with dark margins in live as well as fixed specimens.

Eyes, initially uniserial and monolobate, surround anterior tip. After third millimetre of body, eyes become pluriserially arranged and surrounded by clear halos, spreading onto dorsal surface of body (Fig. 3C–E). Eyes become trilobate behind cephalic region (approximately anterior 1/7th of body); less numerous and uniserially arranged towards posterior tip (Fig. 3C). Diameter of pigment cups 20–40 µm.

*Sensory organs, epidermis and body musculature.* Sensory pits, as simple invaginations (12–20 µm deep), contour cephalic region in a single row (Fig. S3A, B). Creeping sole occupies 93% of body width (Table S3).

Four types of gland discharge through dorsal epidermis and creeping sole of pre-pharyngeal region: rhabditogen cells with xanthophil secretion, two types of cyanophil glands (with amorphous or with fine granular secretion), as well as erythrophil glands with coarse granular secretion (Fig. S3E, F). Glandular margin (Fig. S3C, D), visible posterior to cephalic region, receives four types of gland: abundant glands with coarse, xanthophil secretion, scarcer erythrophil glands producing a fine secretion, and scarce cyanophil glands of two types (with amorphous or fine secretion). Glands discharging through the anterior tip of the body similar to those of the pre-pharyngeal region (Fig. S3B).

Cutaneous musculature with usual three layers (circular, oblique and longitudinal layers), longitudinal layer with thick bundles (Fig. S3C, E, F, Table S4). Index between cutaneous musculature thickness and body height (mc:h 9–15% (Table S4). Thickness of cutaneous musculature gradually diminishes towards anterior tip.

Mesenchymal musculature (Fig. S3C, E, F) well developed, mainly composed of three layers: (1) dorsal subcutaneous, located close to the cutaneous musculature, with oblique decussate fibres (~6–12 fibres thick); (2) supra-intestinal transverse (~10–15 fibres thick); (3) sub-intestinal transverse (~6–8 fibres thick). Mesenchymal musculature thinner in anterior region of body than in the pre-pharyngeal region. *Pharynx*. Cylindrical with dorsal insertion slightly posteriorly displaced (Fig. S3G), 12–14% of body length. Mouth in posterior third of pharyngeal pouch, which shows small posterior diverticulum. Pharynx occupies almost whole length of pharyngeal pouch. Oesophagus short, with folded walls (Fig. S3G). Oesophagus : pharynx ratio 12–16%.

*Reproductive organs.* Testes in one or two irregular rows on either side of body, located beneath dorsal transverse mesenchymal muscles (Fig. S3C, E). Testes begin slightly posteriorly to ovaries, in anterior third of body, and extend to near root of pharynx (Table S3). Sperm ducts dorsal to ovovitelline ducts, sometimes medially displaced (Fig. S3F), forming spermiducal vesicles laterally to pharynx. Spermiducal vesicles extend posteriorly to penis bulb, recurve, ascend and, subsequently, open through lateral walls of forked portion of prostatic vesicle (Fig. 4A, B). Large prostatic vesicle extrabulbar, adjacent to pharyngeal pouch. This vesicle shows

two portions: proximal portion forked, globose, and disposed laterally; distal portion unforked, spacious and funnel shaped (Fig. 4A–C). Ejaculatory duct sinuous, arising from ventro-posterior region of prostatic vesicle and thereafter ascending to open into the antero-dorsal part of male atrium (Fig. 4A–C). Male atrium long, with two differentiated main regions (Fig. 4A, B, Table S3). Proximal region, about anterior 1/10th of male atrium length, obliquely orientated and laterally expanded, presenting numerous small folds (Fig. 4A–C). Distal region of male atrium shows abundant, large folds (Fig. 4A, B).

Vitellaria situated between intestinal branches, well developed in all specimens studied. Ovaries oval–elongate, between two and three times longer than wide, measuring ~0.2 mm in diameter; they are located in anterior fourth of body, dorsally to ventral nerve plate (Table S3). Ovovitelline ducts emerge dorsally from median third of ovaries and run posteriorly immediately above nerve plate (Fig. S3C, F, H). Below female canal, ovovitelline ducts unite to form a common glandular ovovitelline duct (Fig. 4A, B, D). This ascendent duct contours common muscle coat and opens into the posterior-most section of the slightly ventrally flexed female canal (Fig. 4D). The latter shows spacious cavity and penetrates common muscle coat to open into female atrium (postflex condition with ventral approach). The female canal is located dorso-posteriorly to the atrium (Fig. 4A, D). Female atrium oval–elongate with folded wall (Fig. 4A, B). Length of female atrium about half of male atrial length (Fig. S3). Female atrium lined by an epithelium of pseudostratified appearance (Fig. 4D), changing to become columnar and ciliated in the female canal.

Male and female atria with independent muscle coats, with dorsal folds separating their main cavities (Fig. 4A, B). Gonoduct almost vertical at the sagittal plane (Fig. 4A, B).

#### *Type locality*

Salvador do Sul, Rio Grande do Sul (RS), Brazil.

#### *Distribution*

Rio Grande do Sul (Salvador do Sul and Portão), Brazil.

#### *Etymology*

The specific name is a composite of the Latin adjective *albus* (white) and the Latin noun *caudae* (tail), referring to the whitish median stripe, best visible at the posterior tip.

#### ***Pasipha paucilineata* Amaral & Leal-Zanchet, sp. nov.**

<http://zoobank.org/urn:lsid:zoobank.org:act:2D8DC917-6318-4CE5-B1D3-5BB27A1788D1>

#### *Material examined*

*Holotype.* MZUSP PL. 2097: coll. M. H. Sasamori, 23.iii.2014, Portão (29°42'01"S, 50°14'34"W), RS, Brazil – anterior tip: transverse sections on 10 slides; anterior region at the level of the ovaries: sagittal sections on 14 slides; pre-pharyngeal region: transverse sections on 10 slides; pharynx: sagittal sections on 18 slides; copulatory apparatus: sagittal sections on 20 slides.

*Additional material examined.* Collected at the same locality as the holotype, MZU PL. 230: coll. M. H. Sasamori, 27.x.2013 – anterior tip: transverse sections on 18 slides; anterior region at the level of the ovaries in



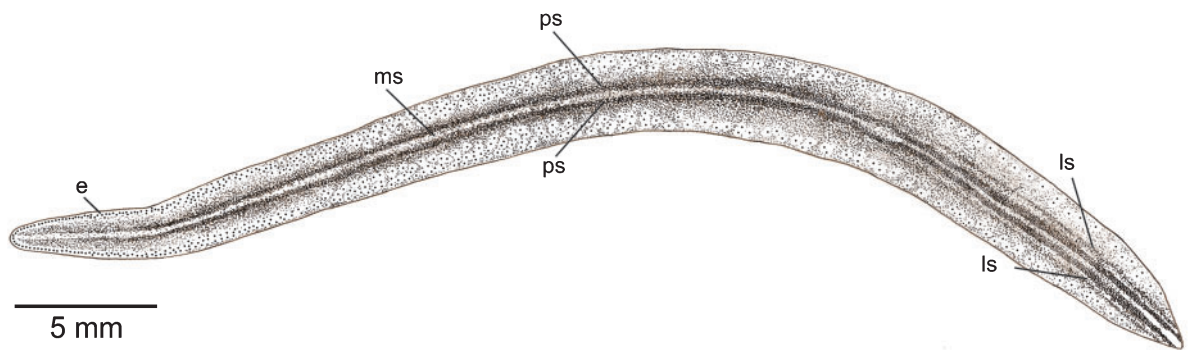
5 mm

(A)



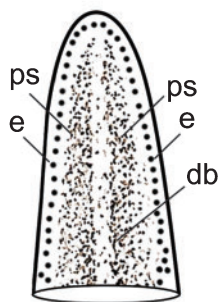
5 mm

(B)



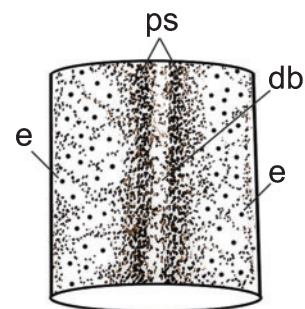
5 mm

(C)



1 mm

(D)



1 mm

(E)

**Fig. 3.** *Pasipha albicaudata*. (A, B) Photographs of live specimens in dorsal view (A: MZU PL. 226; B: holotype). (C) Colour pattern of a fixed specimen (holotype). (D) Detail of eye arrangement in the cephalic region of the holotype. (E) Detail of the median third of the body of the holotype. Anterior tip to the left (A, B) or to the top (C, D).

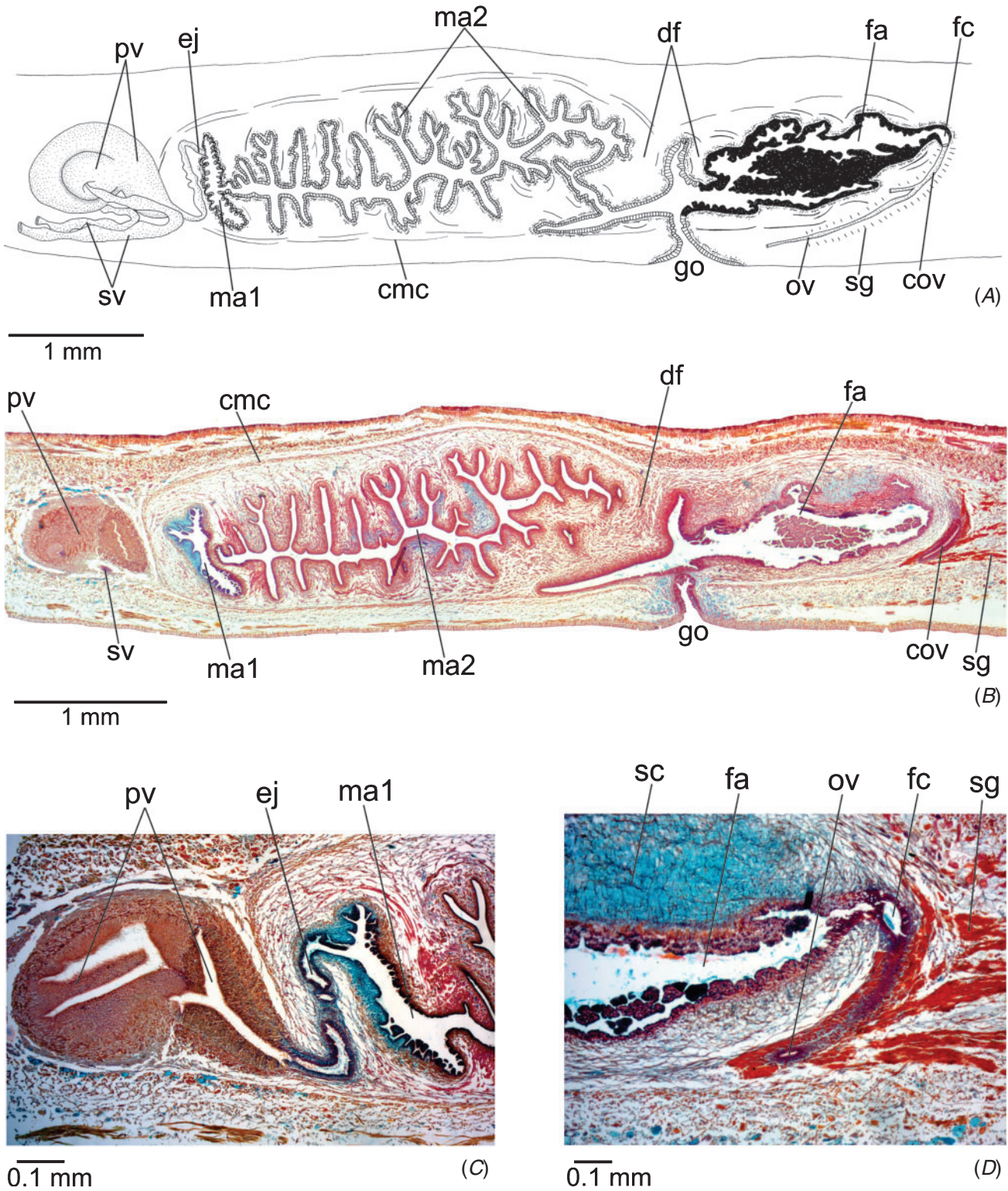


**Fig. 4.** *Pasipha albicaudata*, holotype. (A) Composite reconstruction of the copulatory apparatus from sagittal sections. (B) Microphotograph of the copulatory apparatus in sagittal view. (C) Detail of prostatic vesicle, ejaculatory duct and proximal part of male atrium. (D) Detail of female atrium and female canal. Anterior tip to the left.

two parts: (1) sagittal sections on 11 slides, (2) sagittal sections on 13 slides; pre-pharyngeal region: transverse sections on 13 slides; pharynx: sagittal sections on 21 slides; copulatory apparatus: sagittal sections on 17 slides; MZU PL. 235: coll. M. H. Sasamori, 11.x.2014 – pre-pharyngeal region: transverse sections on 12 slides; pharynx: sagittal sections on 25 slides; copulatory apparatus: sagittal sections on 24 slides; MZU PL. 241: coll. M. H. Sasamori, 18.vii.2015 – copulatory apparatus: horizontal sections on 22 slides.

### Diagnosis

*Pasipha paucilineata* belongs to a group of species with striped colour pattern, eyes spreading over the dorsal surface and cylindrical pharynx, differing from them by epithelium with pseudostratified appearance in female atrium, as well as in anatomical details of the prostatic vesicle. *Pasipha paucilineata* is characterised by prostatic vesicle with proximal portion forked, tubular shaped, and laterally displaced.

### Molecular diagnosis

This species includes all populations that cluster with specimens MZUSP PL. 2097 to MZU PL. 241 (Table S1), with significant support in phylogenetic analyses, as confirmed by species delimitation and following molecular autapomorphies: G(132), C(156), G(174), C(324), C(558), and A(591) (Fig. S1).

### Description

**External features.** Body elongate with parallel margins; anterior tip rounded and posterior tip pointed (Fig. 5A, B). When creeping, maximum length 78 mm. After fixation, maximum length 49 mm. Mouth and gonopore located at posterior third of body (Table S5).

Live animals with dorsal surface black or dark brown (Fig. 5B) with greyish median stripe, more visible under stereomicroscope. After fixation, dorsal colour becomes dark brownish and median stripe more conspicuous (Fig. 5C). Ventral surface pale grey in life and after fixation.

Eyes, initially uniseriate and monolobate, surround anterior tip (Fig. 5C, D). After second millimetre of body, eyes become pluriserially arranged and surrounded by clear halos, spreading onto dorsal surface of body (Fig. 5A, B). Eyes become trilobate behind cephalic region (approximately anterior 1/7th of body; Fig. 5E); less numerous and uniseriate arranged towards posterior tip (Fig. 5C). Diameter of pigment cups 30–60 µm.

**Sensory organs, epidermis and body musculatures.** Sensory pits, as simple invaginations (20–25 µm deep), contour anterior tip and occur ventromarginally in a single row (Fig. S4A, B) in ~1/10th of body. Creeping sole occupies almost whole body width (Supplementary Material Table S5, Fig. S4C, F).

Four gland types discharge through dorsal epidermis and creeping sole of pre-pharyngeal region: abundant erythrophil glands of two types (with coarse and fine granular secretion), rhabditogen cells with xanthophil secretion, and cyanophil glands with amorphous secretion. Glandular margin (Fig. S4C, D), present after cephalic region, receives four types of glands: abundant glands with coarse granular secretion of two types (erythrophil and xanthophil secretions), as well as scarcer glands with erythrophil fine granular secretion and cyanophil glands with amorphous secretion. Glands discharging through

the anterior tip of the body similar to those of pre-pharyngeal region.

Cutaneous musculature with the usual three layers (circular, oblique and longitudinal layers), longitudinal layer with thick bundles (Fig. S4C–F, Table S6). Mc:h 9–13% (Table S6). Thickness of cutaneous musculature gradually diminishes towards anterior tip.

Mesenchymal musculature (Fig. S4A, C, E, F) well developed, mainly composed of three layers: (1) dorsal subcutaneous with oblique decussate fibres (~6–10 fibres thick); (2) supra-intestinal transverse (~4–7 fibres thick); (3) sub-intestinal transverse (~3–7 fibres thick). Mesenchymal musculature thinner in cephalic region than in pre-pharyngeal region.

**Pharynx.** Cylindrical, ~4% of body length, with dorsal insertion slightly posteriorly displaced (Fig. S4G). Mouth in posterior third of pharyngeal pouch, which shows small posterior diverticulum. Pharynx occupies 2/3 of length of pharyngeal pouch. Oesophagus short, with folded walls. Oesophagus: pharynx ratio 13–24%.

**Reproductive organs.** Testes in two or three irregular rows on either side of body, located beneath dorsal transverse mesenchymal muscles (Fig. S4C, E). They begin slightly posteriorly to ovaries, in anterior fourth of the body, and extend laterally to pharynx (Table S5). Sperm ducts medial to ovovitelline ducts (Fig. S4F), forming spermiducal vesicles laterally to pharynx. Distally, spermiducal vesicles extend to penis bulb, turn anteriorly, ascend and open terminally into forked portions of prostatic vesicle (Fig. 6A). Large prostatic vesicle extrabulbar and adjacent to pharyngeal pouch. This vesicle shows two portions: proximal portion forked, tubular shaped, and laterally displaced; distal portion unforked, spacious and oval–elongate with folded walls (Fig. 6A–D). Ejaculatory duct sinuous, arising from ventro-posterior region of prostatic vesicle and ascending to open into the antero-dorsal part of male atrium (Fig. 6A, C). Male atrium long, with two differentiated main regions (Table S5, Fig. 6A, B). Proximal region, about anterior 1/6 of male atrium length, presents numerous small folds. Distal region of male atrium shows abundant, large folds that narrow the whole cavity (Fig. 6A, B).

Vitellaria, situated between intestinal branches, well developed in holotype and in specimen MZU PL. 241. Ovaries oval–elongate, between four and five times longer than wide, measuring 0.2 mm in diameter. They are located dorsally to the ventral nerve plate, in anterior third of body (Table S5). Ovovitelline ducts emerge dorsally from posterior half of ovaries and run medially ventrally to proximal third of female atrium. Common glandular ovovitelline duct slightly ascendant, contouring the common muscle coat, below the female canal, to open into ental portion of this canal. Female canal almost vertical and located posteriorly to female atrium. Female atrium oval–elongate and highly folded, showing a length of about one-third of male atrial length (Fig. 6A, B, Table S5). Female atrium lined by epithelium of pseudostratified appearance exhibiting irregular height and multilayered aspect. Female canal lined by ciliated, columnar epithelium.

Male and female atria with independent muscle coats. Dorsal folds separate male and female atria. Gonoduct slightly inclined forward at the sagittal plane (Fig. 6A, B).

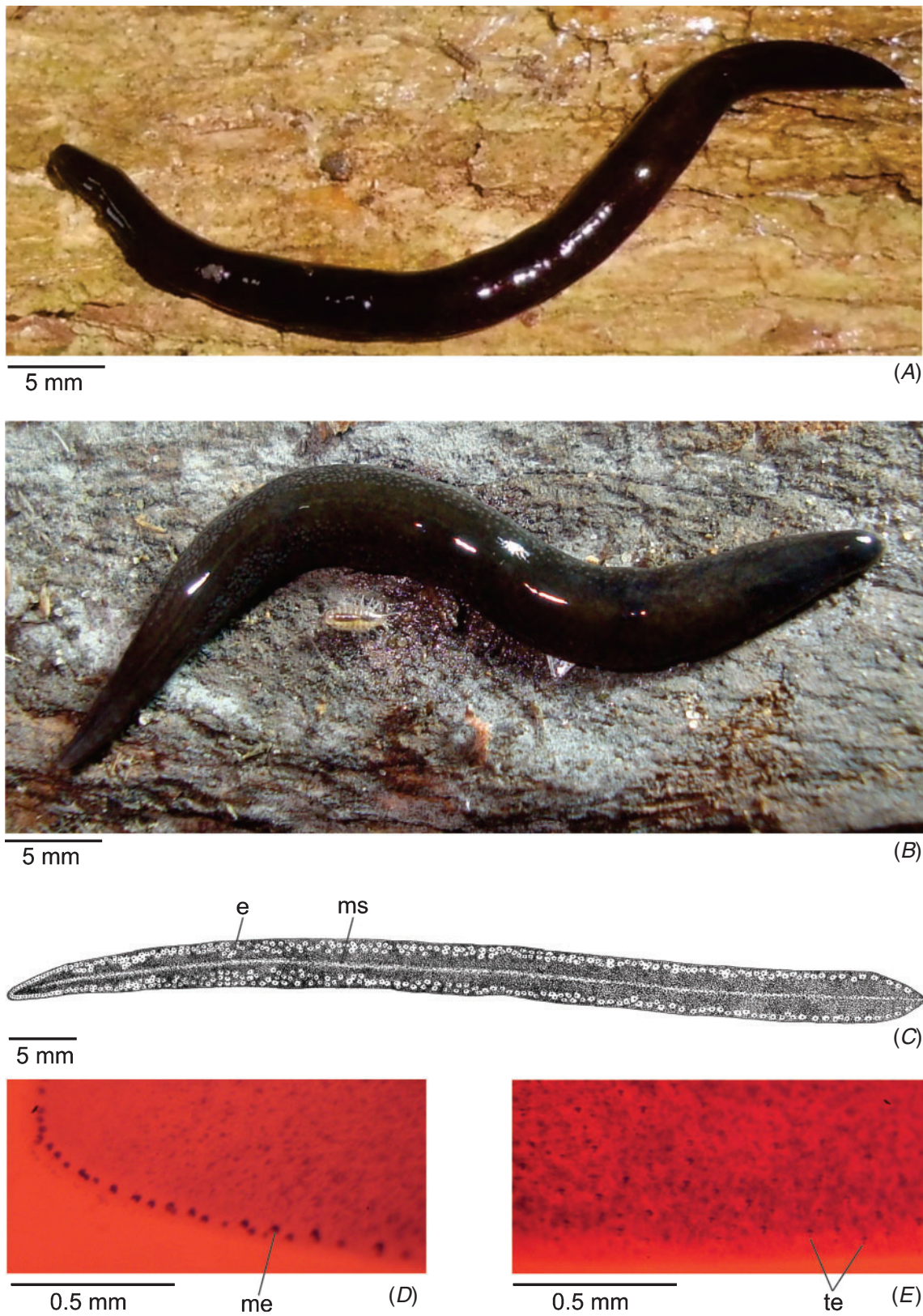


**Fig. 5.** *Pasipha paucilineata*. (A, B) Photographs of live specimens in dorsal view (A: holotype; B: MZU PL. 241). (C) Colour pattern of a fixed specimen (MZU PL. 235) in dorsal view. (D) Photograph of monolobate eyes in clove oil. (E) Photograph of trilobate eyes in clove oil (D, E: MZU PL. 235).

*Type locality*

Portão, state of Rio Grande do Sul (RS), Brazil.

*Distribution*

Known only from its type locality.

*Etymology*

The specific name is a composite of the Latin adjective *paucus* (minimal) and the Latin noun *linea* (stripe) and refers to the median stripe, sometimes indistinct to naked eye.

*Remarks*

Specimens MZU PL. 230 and MZU PL. 235 were not fully mature, showing poorly developed vitellaria and testes; copulatory apparatus was not developed in the latter.

***Pasipha variistriata* Amaral & Leal-Zanchet, sp. nov.**

<http://zoobank.org/urn:lsid:zoobank.org:act:1351A74D-15DA-4CB8-AB87-123DADDBB495>

*Material examined*

*Holotype.* MZUSP PL. 2098: coll. S. V. Amaral, 26.x.2014, Araucaria Natural Heritage Private Reserve (26°23'53.53"S, 51°24'15.96"W), General Carneiro, Paraná (PR), Brazil – anterior tip: transverse sections on 20 slides; anterior region at the level of the ovaries: sagittal sections on 36 slides; pre-pharyngeal region: transverse sections on 14 slides; pharynx: sagittal sections on 37 slides; copulatory apparatus: sagittal sections on 75 slides.

*Additional material examined.* Collected at the same locality as the holotype – MZU PL. 243: coll. I. Rossi, 18.vii.2014 – anterior tip: transverse sections on 15 slides; anterior region at the level of the ovaries: sagittal sections on 60 slides; pre-pharyngeal region: transverse sections on 17 slides; pharynx: sagittal sections on 16 slides; copulatory apparatus: sagittal sections on 44 slides; MZU PL. 248: coll. I. Rossi, 19.vii.2014 – pre-pharyngeal region: transverse sections on 15 slides; pharynx and copulatory apparatus: sagittal sections on 70 slides; MZU PL. 250: coll. I. Rossi, 25.x.2014 – copulatory apparatus: horizontal sections on 65 slides; MZU PL. 245: coll. I. Rossi, 18.vii.2014 – preserved in ethyl alcohol.

*Diagnosis*

*Pasipha variistriata* Amaral & Leal-Zanchet, sp. nov. belongs to group of species with striped colour pattern, eyes spreading over dorsal surface and cylindrical pharynx, differing from them by epithelium with pseudostratified appearance in female atrium, as well as in anatomical details of prostatic vesicle. *Pasipha variistriata* shows prostatic vesicle with proximal portion forked and tubular shaped, almost horizontal and located anteriorly to main portion.

*Molecular diagnosis*

This species includes all populations that cluster with specimens MZUSP PL. 2098 to MZU PL. 252 (Table S1), with significant support in phylogenetic analyses, as established by species delimitation tools and following molecular autapomorphies: T(6), A(48), T(78), G(136), G(141), A(156), C(195), T(252), A(363), A(372), A(405), and A(645) (Fig. S1).

*Description*

*External features.* Body elongate with parallel margins; anterior tip rounded and posterior tip pointed (Fig. 7A–D). When creeping, maximal length 85 mm. After fixation, maximum length 72 mm. Mouth and gonopore located in posterior third of body (Table S7).

Live specimens with dorsal surface varying from dark brown to light brown; pale yellow median stripe, visible in anterior third and posterior tip of body (Fig. 7A). Some specimens with median stripe bordered by dark pigmentation (Fig. 7B). Additionally, specimens may have two black lateral stripes (Fig. 7C). After fixation, dorsal colour dark brown and median stripe occurring along body length (Fig. 7D). Ventral surface pale grey with dark margins in live and fixed specimens.

Eyes, uniseriably arranged and monolobate, surround anterior tip. Two millimetres behind the tip, eyes become pluriseriably arranged and are surrounded by clear halos, spreading onto dorsal surface of body (Fig. 7D). Eyes become trilobate behind cephalic region (approximately first 1/7th of body); less numerous and uniseriably arranged towards posterior tip (Fig. 7D). Diameter of pigment cups 20–30 µm.

*Sensory organs, epidermis and body musculature.* Sensory pits, being simple invaginations (25–30 µm deep), contour anterior tip and occur ventromarginally in single row in anterior 1/14th of body. Creeping sole occupies whole body width (Table S7, Fig. S5A, D).

Five types of gland discharge through dorsal epidermis and creeping sole of pre-pharyngeal region: rhabditogen cells with xanthophil secretion, cyanophil glands of two types (with coarse granular or amorphous secretion), as well as erythrophil glands of two types (with coarse or fine granular secretion). Glandular margin, present after cephalic region, receives four types of glands (Fig. S5A, B): abundant erythrophil glands of two types (with coarse granules or fine granules), as well as cyanophil glands of two types (with amorphous secretion or fine granular secretion). Glands discharging through anterior tip of body are similar to those of pre-pharyngeal region.

Cutaneous musculature with the usual three layers (circular, oblique and longitudinal layers), longitudinal layer with thick bundles (Fig. S5A–D, Table S8). Mc:h 11–12% (Table S8). Thickness of cutaneous musculature gradually diminishes towards anterior tip.

Mesenchymal musculature (Fig. S5A, C, D) well developed, mainly composed of three layers: (1) dorsal subcutaneous with oblique decussate fibres (~20–25 fibres thick); (2) supra-intestinal transverse (~8–15 fibres thick); (3) sub-intestinal transverse (~8–16 fibres thick). Mesenchymal musculature thinner in cephalic region than in pre-pharyngeal region.

*Pharynx.* Cylindrical, ~3% of the body length, with dorsal insertion slightly posteriorly shifted (Fig. S5E). Mouth in posterior third of pharyngeal pouch, which shows small posterior diverticulum. Pharynx occupies almost whole length of pharyngeal pouch. Oesophagus with slightly folded walls (Fig. S5E). Oesophagus : pharynx ratio 26–43%.

*Reproductive organs.* Testes in two or three irregular rows on either side of the body, located beneath dorsal transverse mesenchymal muscles (Fig. S5A, C), begin posteriorly to ovaries, in anterior third of body, and extend to near root of pharynx

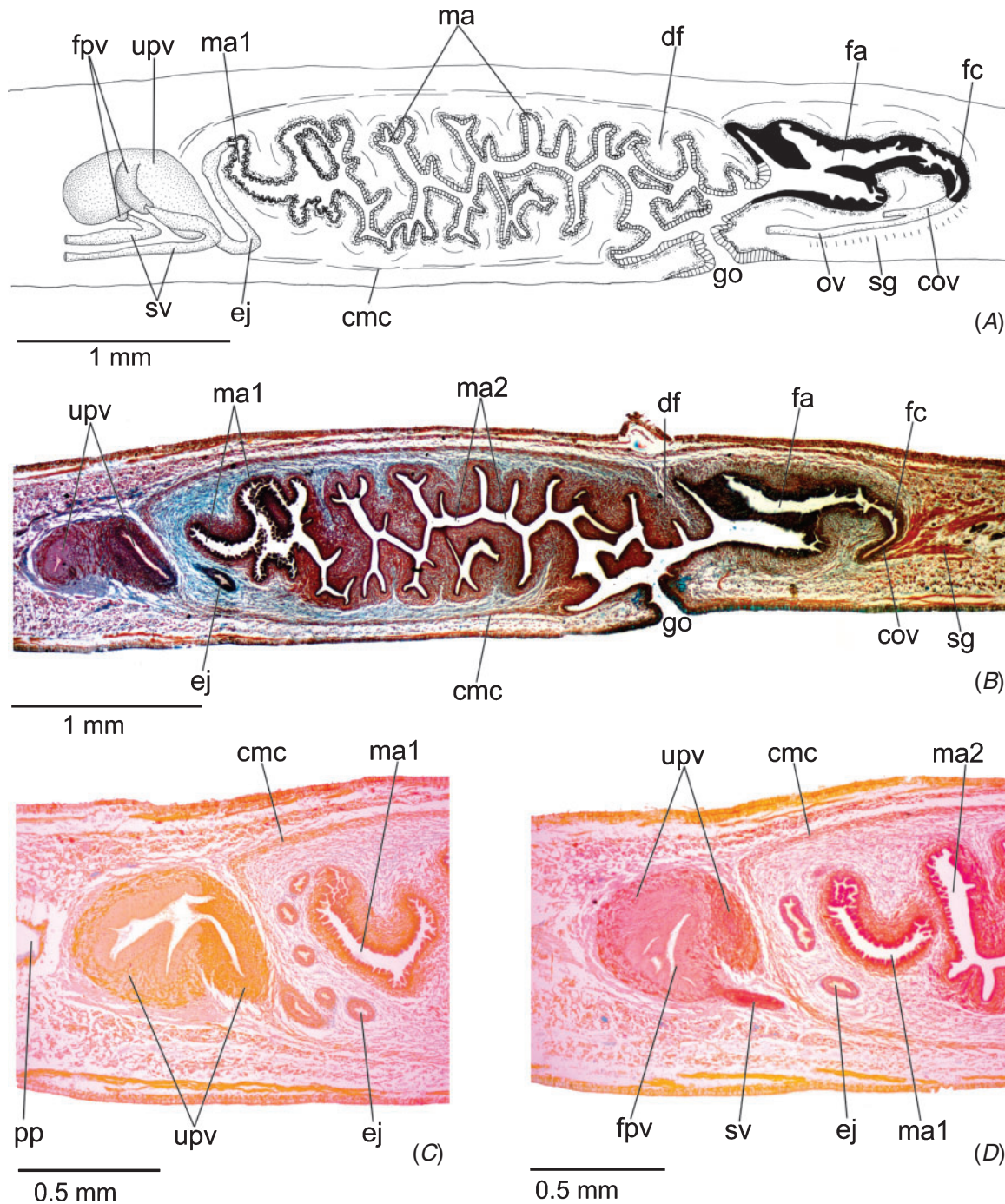


**Fig. 6.** *Pasipha paucilineata*, holotype. (A) Composite reconstruction of the copulatory apparatus from sagittal sections. (B) Microphotograph of the copulatory apparatus in sagittal view. (C) Detail of prostatic vesicle in sagittal section. (D) Detail of prostatic vesicle and opening of spermiducal vesicle in sagittal section. Anterior tip to the left.

(Table S8). Sperm ducts dorsal to ovovitelline ducts (Fig. S5D), forming spermiducal vesicles posteriorly to pharynx. Spermiducal vesicles extend to penis bulb, recurve, ascend and open terminally into lateral branches of prostatic vesicle (Fig. 8A, C). Large prostatic vesicle extrabulbar and adjacent to pharyngeal pouch. This vesicle shows two portions: anterior portion forked and tubular, almost horizontal

and posteriorly inclined; posterior portion unforked, with spacious ental half and funnel shaped ectal half, giving an oval elongated shape to this main portion of the vesicle (Fig. 8A–C). Ejaculatory duct sinuous, arising from postero-ventral section of prostatic vesicle and subsequently ascending to open into anterodorsal part of male atrium (Fig. 8A). Male atrium long, with two main regions (Table S7, Fig. 8A, B). Proximal region of male



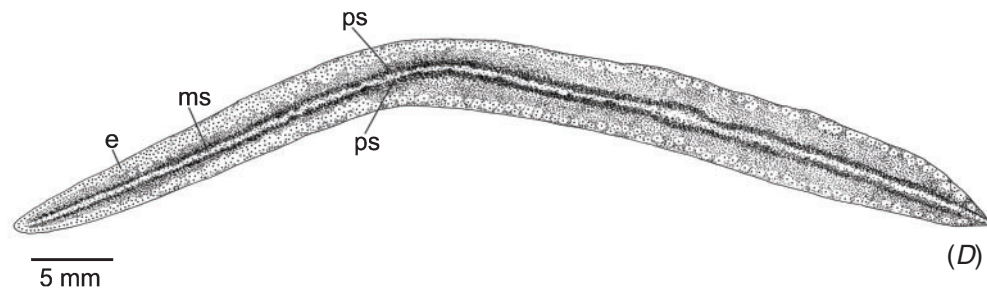
(A)



(B)



(C)



(D)

**Fig. 7.** *Pasipha variistriata*. (A–C) Photographs of live specimens in dorsal view (A: holotype; B: MZU PL. 243; C: MZU PL. 245). (D) Colour pattern of a fixed specimen (MZU PL. 243). Anterior tip to the left.

atrium, about anterior 1/3rd of male atrium length, horizontally disposed and laterally expanded, with numerous small folds. Distal region of male atrium shows abundant, large folds that narrow the whole cavity (Fig. 8A, B).

Vitellaria, situated between intestinal branches, well developed in the holotype and specimen MZU PL. 250. Ovaries oval–elongate (Fig. S5F), three times longer than wide, measuring 0.2 mm in diameter; they are situated dorsally to ventral nerve plate, in anterior fourth of body (Table S7). Ovovitelline ducts emerge dorsally from median third of ovaries (Fig. S5F) and run posteriorly immediately above nerve plate. Posteriorly to gonopore, ovovitelline ducts run medially and, ventrally to female canal, they unite to form a common glandular ovovitelline duct. The latter is almost vertical, contouring the common muscle coat, to open into posterior portion of the female canal. Female canal almost horizontal and located postero-dorsal to female atrium. Female atrium oval–elongate and folded (Fig. 8A, B, D, Table S7). Length of female atrium about two-thirds of male atrial length. Female atrium lined by epithelium of pseudostratified appearance exhibiting irregular height. Female canal lined by ciliated, columnar epithelium (Fig. 8D).

Male and female atria with independent muscle coats, comprising longitudinal, oblique and circular fibres (Fig. 8A, B). Dorsal folds separate male and female atria, which communicate with gonoduct in different planes (Fig. 8A, B). Gonoduct vertical at the sagittal plane (Fig. 8A, B).

#### Type locality

General Carneiro, Paraná, Brazil.

#### Distribution

Known from its type locality.

#### Etymology

The specific name refers to the variable number of stripes in different specimens, being a composite of the Latin adjective *variatus* (variable) and the Latin noun *striatus* (striped).

#### Remarks

Specimens MZU PL. 243 and MZU PL. 248 were not fully mature, showing poorly developed vitellaria and few shell glands.

### *Pasipha* sp.

#### Material examined

São Leopoldo, RS, Brazil, MZU PL. 253: *leg.* L. Negrete, 28.x.2013 (29°47'2.37"S, 51°9'7.21"W) – pre-pharyngeal region: transverse sections on 11 slides; pharynx: sagittal sections on 14 slides; posterior region of the body: sagittal sections on 25 slides; MZU PL. 254: *leg.* L. Negrete, 28.x.2013 (29°47'2.37"S, 51°9'7.21"W) – posterior region of the body: sagittal sections on 33 slides; MZU PL. 255: *leg.* L. Negrete, 28.x. 2013 (29°47'2.37"S, 51°9'7.21"W) – preserved in ethyl alcohol; MZU PL. 256: *leg.* J. Braccini, 12.vii.July 2014 (29°45'0.29"S, 51°3'42.68"W) – preserved in ethyl alcohol.

#### Description

Body elongate with parallel margins, anterior tip rounded and posterior tip pointed (Fig. S6A). When creeping, maximum length 62 mm. After fixation, maximum length 37 mm. Mouth

located in posterior third of body (Table S9). Gonopore absent in the specimens analysed.

Live animals with dorsal surface brown (Fig. S6A, B) presenting a pale yellow median stripe. Specimen MZU PL. 253 has inconspicuous median stripe, which becomes broader and whitish on posterior tip of body (Fig. S6A). After fixation, dorsal colour becomes dark brownish. Ventral surface pale grey in both live and fixed specimens.

Eyes, initially uniserial and monolobate, surround anterior tip. Three millimetres behind the tip, eyes become pluriserially arranged and are surrounded by clear halos, spreading onto dorsal surface of body. Eyes become trilobate behind cephalic region (approximately anterior 1/7th of body); less numerous and uniserially arranged towards posterior tip. Diameter of pigment cups 15–30 µm.

Creeping sole occupies whole body width. Three types of gland discharge through dorsal epidermis and creeping sole of pre-pharyngeal region: numerous rhabditogen cells with xanthophil secretion, erythrophil glands with coarse granular secretion and cyanophil glands with amorphous secretion. Erythrophil glands are more abundant in the dorsal epidermis than in the creeping sole. Glandular margin constituted by three types of gland: erythrophil and xanthophil glands, both with coarse granular secretion, as well as cyanophil glands with amorphous secretion.

Cutaneous musculature with the usual three layers (circular, oblique and longitudinal layers), longitudinal layer with thick bundles. Dorsal musculature thicker than ventral at the sagittal plane. Mc:h 12% (Table S10).

Mesenchymal musculature well developed, mainly composed of three layers: (1) dorsal subcutaneous with oblique decussate fibres (~3–6 fibres thick); (2) supra-intestinal transverse (~3–5 fibres thick); (3) sub-intestinal transverse (~2–4 fibres thick).

Pharynx cylindrical, ~5% of body length. Mouth at median third of pharyngeal pouch, which shows a posterior diverticulum. Pharynx occupies ~2/3 of pharyngeal pouch length. Oesophagus short, with folded walls. Oesophagus : pharynx ratio 24%.

Copulatory organs not developed in the specimens analysed.

### Comparative discussion

The integrative approach indicates that the four studied taxa belong to the genus *Pasipha* and constitute independent evolutionary units. Comparisons of the new species with their congeners using intraspecific and interspecific variations of the *COI* gene, as well as the methods for species delimitation and the analysis of autapomorphies, are congruent with the results of the morphological analyses. Thus, the three new species herein described present characteristics that conform to the diagnosis of the genus *Pasipha*, such as an elongate body with parallel margins and prostatic vesicle with two portions receiving different secretions (Carbayo *et al.* 2013). They also show a folded male atrium separated from the female atrium by dorsal fold(s), and a ventrally flexed female canal, located in the posterior region of the female atrium (i.e. a post-flex condition with ventral approach). Such morphological characteristics of the reproductive organs could not be confirmed in *Pasipha* sp., which was represented only by immature specimens in the examined material, thus being considered an unconfirmed

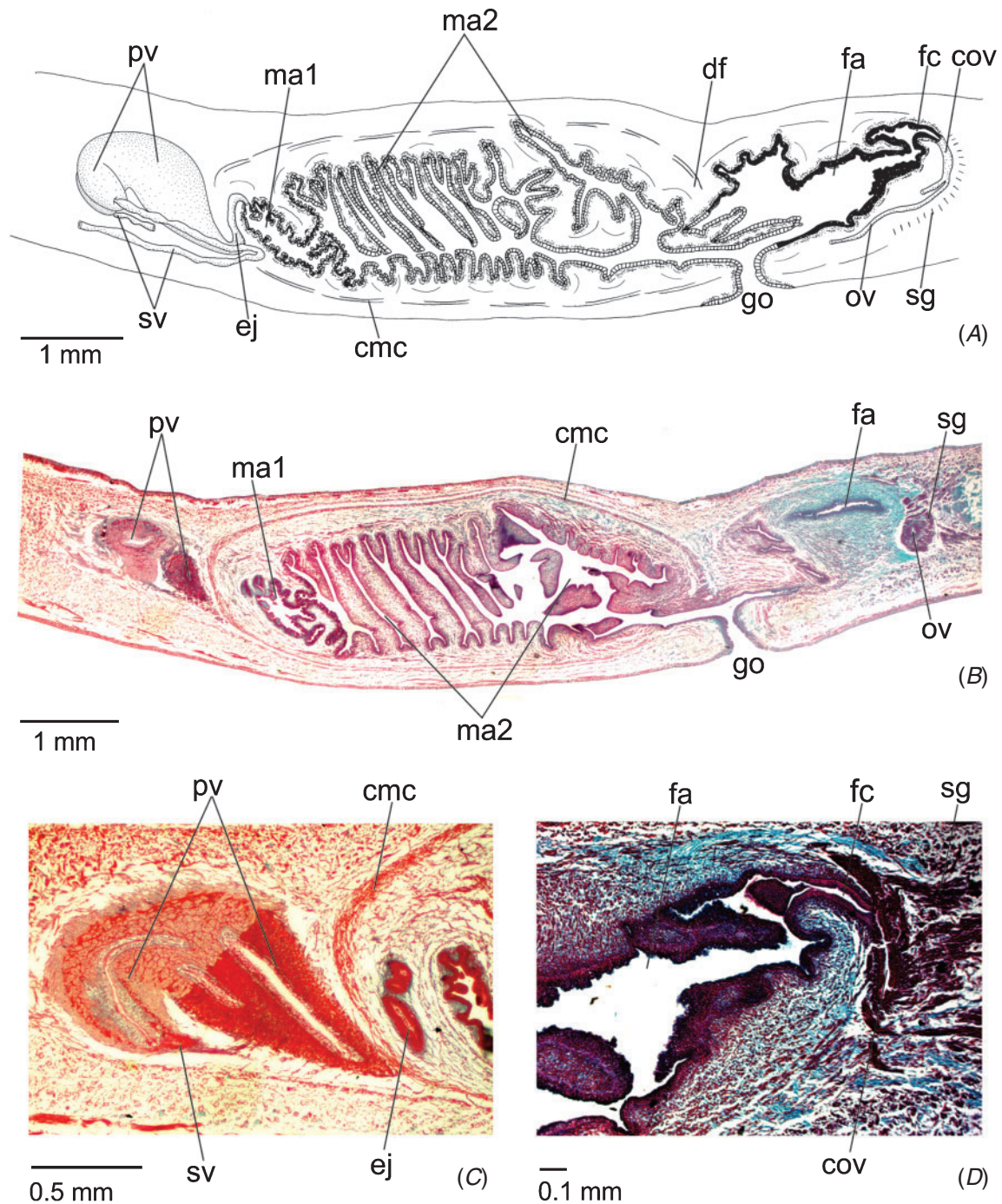


**Fig. 8.** *Pasipha variistriata*, holotype. (A) Composite reconstruction of the copulatory apparatus from sagittal sections. (B) Microphotograph of the copulatory apparatus in sagittal view. (C) Detail of prostatic vesicle and spermiducal vesicle. (D) Detail of female atrium, female canal and common ovovitelline duct. Anterior tip to the left.

candidate species. However, other aspects, such as body shape, eye morphology and arrangement, as well as thickness and arrangement of body musculatures, among others, match those described for other species of *Pasipha* (Leal-Zanchet *et al.* 2012; Amaral & Leal-Zanchet 2016; Negrete and Brusa 2016).

The new species herein described share similarities with no less than 10 species of the genus, namely the type species,

*Pasipha pasipha* (Marcus, 1951), as well as *Pasipha pinima* (E.M. Froehlich, 1955), *Pasipha tapetilla* (Marcus, 1951), *Pasipha backesi* Leal-Zanchet, Rossi & Seitenfus, 2012, *Pasipha brevilineata* Leal-Zanchet, Rossi & Alvarenga, 2012, *Pasipha atla* Negrete & Brusa, 2016, *Pasipha johnsoni* Negrete & Brusa, 2016, *Pasipha mbya* Negrete & Brusa, 2016, *Pasipha mesoxantha* Amaral & Leal-Zanchet, 2016 and *Pasipha turvensis*

Amaral & Leal-Zanchet, 2016. All of these species have eyes spreading over the dorsal surface as well as a cylindrical pharynx (Marcus 1951; Froehlich 1955; Leal-Zanchet *et al.* 2012; Amaral and Leal-Zanchet 2016; Negrete and Brusa 2016). Therefore, in the following comparative discussion we discuss these species in relation to the new species.

Regarding colour pattern, by having a median stripe and two irregular lateral stripes, *P. albicaudata* differs from *P. pinima*, which shows a homogeneous pattern, as well as from *P. tapetilla*, *P. backesi* and *P. johnsoni*, which exhibit continuous lateral stripes (Marcus 1951; Froehlich 1955; Leal-Zanchet *et al.* 2012; Negrete and Brusa 2016). It can be distinguished also from *P. pasipha*, *P. brevilineata* and *P. atla*, as these species show only a whitish median stripe that is restricted to the cephalic and posterior region of the body in *P. atla* (Marcus 1951; Leal-Zanchet *et al.* 2012; Negrete and Brusa 2016). *Pasipha albicaudata* differs from *P. mesoxantha* and *P. mbya* because these species show a yellowish median band, as well as from *P. turvensis*, which shows a whitish median band bordered by black paramedian stripes. *Pasipha paucilineata* has a dark dorsal surface with a greyish median stripe, thus differing from *P. albicaudata* and the other species mentioned above. *Pasipha variistriata* has a pale yellow median stripe on the anterior third and the posterior tip of the body on a dorsal ground colour varying from dark brown to light brown. Some specimens show a median stripe bordered by dark pigmentation or two black lateral stripes. Since it has a striped, but variable dorsal pattern, *P. variistriata* can be differentiated only from *P. pinima*, which shows a homogeneous pattern.

With respect to internal anatomy, *P. albicaudata*, *P. paucilineata* and *P. variistriata* show an epithelium with stratified appearance lining the female atrium, thus differing from all remaining species of this group, which show a columnar epithelium. The three new species have a large prostatic vesicle with proximal forked portions, and thus differs from that of *P. tapetilla* and *P. pinima*, which is unforked.

*Pasipha albicaudata* has globose forked portions in its prostatic vesicle, different from *P. brevilineata*, *P. atla*, *P. turvensis*, *P. paucilineata* and *P. variistriata*, in which the forked portions are tubular. *Pasipha albicaudata* can be distinguished also from *P. pasipha*, *P. backesi*, *P. johnsoni*, *P. mbya* and *P. mesoxantha*, in which the forked portions are globose, but located anteriorly to the main portion (= distal portion) of the vesicle, whereas in *P. albicaudata* the forked portions are disposed laterally to the main portion.

*Pasipha paucilineata* has tubular forked portions in the prostatic vesicle, similar to *P. brevilineata*, *P. atla*, *P. turvensis* and *P. variistriata*, but these portions are laterally displaced in *P. paucilineata*, in contrast to the other species, in which the forked portions are located anteriorly to the main portion of the vesicle. Furthermore, the main portion of the vesicle is oval–elongate in *P. paucilineata*, whereas in *P. atla* and *P. turvensis* it is funnel shaped (Leal-Zanchet *et al.* 2012; Negrete and Brusa 2016; Amaral and Leal-Zanchet 2016).

In *P. variistriata*, the forked portions of the prostatic vesicle are similar to those of *P. brevilineata*, *P. atla* and *P. turvensis*, i.e. tubular shaped and located anteriorly to the main portion of the vesicle. However, the forked portions of the prostatic vesicle are almost horizontal and posteriorly inclined in *P. variistriata*,

whereas they are almost vertical in *P. brevilineata*. *Pasipha variistriata* cannot be differed from *P. atla* and *P. turvensis* by the anatomy of the forked portions of the prostatic vesicle, but, having the main portion of the prostatic vesicle oval–elongate, it thus differs from that of *P. atla* and *P. turvensis*, which is tubular.

Thus, the three new species herein described have similar external features, and they differ anatomically only in slight details of their prostatic vesicles. When compared with recently described species that have more detailed morphological descriptions, other differential characteristics are noticeable. The glandular margin is absent in *P. atla* and *P. johnsoni*, but it is present in *P. backesi*, *P. brevilineata*, *P. mbya*, *P. mesoxantha*, *P. turvensis* and in the new species. The ejaculatory duct opens into the antero-dorsal part of the male atrium in the three new species, as well as in *P. brevilineata*, *P. johnsoni*, *P. mesoxantha* and *P. turvensis*. In contrast, in *P. atla* the opening of the ejaculatory duct occurs into the antero-ventral part of the male atrium, whereas in *P. backesi* and *P. mbya*, there is neither ventral nor dorsal displacement regarding the opening of this duct into the atrium. The three species described from Argentina, *P. atla*, *P. johnsoni* and *P. mbya*, have an ovoid female atrium with few folds, while in the three Brazilian species the female atrium is oval–elongate and highly folded. Furthermore, *P. albicaudata*, *P. paucilineata* and *P. variistriata* are the only species having the female atrium lined by an epithelium of pseudostratified appearance, whereas in other species the female atrium is lined by a columnar epithelium.

#### Notes on ecology and distribution

All species studied were found in human-disturbed areas. *Pasipha albicaudata* and *Pasipha paucilineata*, as well as *Pasipha* sp., occur in urban, unprotected areas of north-east hillsides of Rio Grande do Sul (southern Brazil). *Pasipha paucilineata* was found only in Portão city, being sympatric with *P. albicaudata* in this area. *Pasipha variistriata* was found only in a protected area, namely the Araucaria Natural Heritage Private Reserve, located ~500 km north from the other studied areas. This reserve harbours sites of mixed ombrophilous forest showing an initial stage of regeneration, with poorly developed understory, and plantations of the exotic *Pinus elliotii*.

#### General discussion

Delimiting species within *Pasipha* has been problematic due to its anatomical homogeneity (Leal-Zanchet *et al.* 2012; Amaral and Leal-Zanchet 2016; Negrete and Brusa 2016). Despite that, until now, an integrative approach has not been used to disentangle species within this genus. In many cases, external features, namely colour pattern and eye arrangement, have been very helpful in differentiating species of *Pasipha* (Leal-Zanchet *et al.* 2012; Negrete and Brusa 2016). However, the use of external features is not possible in the case of the striped species herein studied, which have a pattern similar to *P. brevilineata*, another southern Brazilian species. The slight differences in the anatomy of the prostatic vesicle of the three species and *P. brevilineata* are difficult to be interpreted as representing interspecific variations without the support of molecular data.

Thus, the use of the integrative method in the present study was essential to detect species boundaries and results indicate that we are dealing with sibling species.

In a molecular approach to the subfamily Geoplaninae, only five species of *Pasipha* were studied (Carbayo *et al.* 2013). Herein we present the first integrative taxonomic approach for species of this genus and add molecular data for another five species, including the three new species herein described and two already known species (*P. brevilineata* and *P. hauseri* Froehlich, 1959), all of them from southern Brazil. Since the studied species show a more southern distribution than the previously studied species, knowledge on the geographic and genetic divergence within *Pasipha* is enhanced.

The mean interspecific distance (9.3%) for the *Pasipha* species of the present study is similar to the mean interspecific divergence (11.7%) obtained for species of two other genera of Geoplaninae in a previous study using DNA barcoding (Rossi *et al.* 2015). Regarding intraspecific divergence, *Pasipha chimbeva* constituted an exception (5.4%), similarly to *Imbira marcusii*, indicating that each nucleotide sequence deposited in GenBank identified as *P. chimbeva* and *I. marcusii*, respectively, correspond to evolutionarily independent species (Amaral *et al.* 2018). It should be noted that overestimations under the GMYC approach have been observed in previous studies (Puillandre *et al.* 2012; Talavera *et al.* 2013). However, our results, estimated by PTP approach from RAXML tree, as well as the partition output by ABGD, showed similar results to those of the GMYC analysis (see also Lang *et al.* 2015). Therefore, we do not consider these results to be an overestimation of the number of putative species and we suggest that the specific status of specimens of *P. chimbeva* and *I. marcusii* available in GenBank should be reviewed. An integrative taxonomic approach, as done for the three new species herein proposed, may resolve this issue.

## Conflicts of interest

The authors declare no conflicts of interest.

## Acknowledgements

We gratefully acknowledge the Conselho Nacional de Desenvolvimento Científico e Tecnológico (CNPq) and the Coordenação de Aperfeiçoamento de Pessoal de Nível Superior (CAPES) for research grants and fellowships in support of this study. The Instituto Chico Mendes de Conservação da Biodiversidade is acknowledged for collection licence permits (SISBIO 24357-1). We acknowledge I. Rossi, J. A. L. Braccini, L. Negrete and M. H. Sasamori for their help in sampling flatworms, as well as I. Rossi for the photos of *Pasipha variistriata* in the figures 7B and 7C. We also thank Dr M. Müller and H. Allgayer for their support in the analyses and valuable comments on an early draft of the manuscript. MSc. Edward Benya is acknowledged for an English review of the manuscript. Dr Fernando Carbayo (USP) and two anonymous reviewers are thanked for valuable suggestions on an early draft of the manuscript.

## References

- Akaike, H. (1974). A new look at the statistical model identification. *IEEE Transactions on Automatic Control* **19**, 716–723. doi:10.1109/TAC.1974.1100705
- Álvarez-Presas, M., Carbayo, F., Rozas, J., and Riutort, M. (2011). Land planarians (Platyhelminthes) as a model organism for fine scale phylogeographic studies: understanding patterns of biodiversity in the Brazilian Atlantic Forest hotspot. *Journal of Evolutionary Biology* **24**, 887–896. doi:10.1111/j.1420-9101.2010.02220.x
- Álvarez-Presas, M., Amaral, S. V., Carbayo, F., Leal-Zanchet, A. M., and Riutort, M. (2015). Focus on the details: morphological evidence supports new cryptic land flatworm (Platyhelminthes) species revealed with molecules. *Organisms, Diversity & Evolution* **15**, 379–403. doi:10.1007/s13127-014-0197-z
- Amaral, S. V., and Leal-Zanchet, A. M. (2016). Two new species of land flatworms *Pasipha* Ogren & Kawakatsu (Platyhelminthes: Continenticola) from areas of caducifolious deciduous forest in southern Brazil. *Zootaxa* **4171**(3), 459–474. doi:10.11646/zootaxa.4171.3.3
- Amaral, S. V., Ribeiro, G. G., Müller, M. J., Valiati, V. H., and Leal-Zanchet, A. (2018). Tracking the diversity of the flatworm genus *Imbira* (Platyhelminthes) in the Atlantic Forest. *Organisms, Diversity & Evolution*. doi:10.1007/s13127-018-0358-6
- Bickford, D., Lohman, D. J., Sodhi, N. S., Ng, P. K. L., Meier, R., Winker, K., Ingram, K. K., and Das, I. (2007). Cryptic species as a window on diversity and conservation. *Trends in Ecology & Evolution* **22**(3), 148–155. doi:10.1016/j.tree.2006.11.004
- Bouckaert, R., Heled, J., Kühnert, D., Vaughan, T., Wu, C.-H., Xie, D., and Drummond, A. J. (2014). BEAST 2: a software platform for Bayesian evolutionary analysis. *PLoS Computational Biology* **10**(4), e1003537. doi:10.1371/journal.pcbi.1003537
- Carbayo, F., Álvarez-Presas, M., Olivares, C. T., Marques, F. P. L., Froehlich, E. M., and Riutort, M. (2013). Molecular phylogeny of Geoplaninae (Platyhelminthes) challenges current classification: proposal of taxonomic actions. *Zoologica Scripta* **42**, 508–528. doi:10.1111/zsc.12019
- Carbayo, F., Álvarez-Presas, M., Jones, H. D., and Riutort, M. (2016). The true identity of *Obama* (Platyhelminthes: Geoplanidae) flatworm spreading across Europe. *Zoological Journal of the Linnean Society* **177**, 5–28. doi:10.1111/zoj.12358
- Darriba, D., Taboada, G. L., Doallo, R., and Posada, D. (2012). jModelTest 2: more models, new heuristics and parallel computing. *Nature Methods* **9**, 772. doi:10.1038/nmeth.2109
- Felsenstein, J. (1985). Confidence limits on phylogenies: an approach using the bootstrap. *Evolution* **39**, 783–791. doi:10.1111/j.1558-5646.1985.tb00420.x
- Frankham, R., Ballou, J. D., Dudash, M. R., Eldridge, M. D. B., Fenster, C. B., Lacy, R. C., Mendelson, J. R. III, Porton, I. J., Ralls, K., and Ryder, O. A. (2012). Implications of different concepts for conserving biodiversity. *Biological Conservation* **153**, 25–31. doi:10.1016/j.biocon.2012.04.034
- Froehlich, E. M. (1955). Sobre espécies brasileiras do gênero *Geoplana*. *Boletim da Faculdade de Filosofia, Ciências e Letras da Universidade de São Paulo. Série Zoologia* **19**, 289–369.
- Fujisawa, T., and Barraclough, T. G. (2013). Delimiting species using single-locus data and the Generalized Mixed Yule Coalescent approach: a revised method and evaluation on simulated data sets. *Systematic Biology* **62**(5), 707–724. doi:10.1093/sysbio/syt033
- Guindon, M., and Gascuel, O. (2010). SeaView version 4: a multiplatform graphical user interface for sequence alignment and phylogenetic tree building. *Molecular Biology and Evolution* **27**(2), 221–224. doi:10.1093/molbev/msp259
- Hall, T. A. (1999). BioEdit: a user-friendly biological sequences alignment editor and analysis program for Windows 95/98 NT. *Nucleic Acids Symposium Series* **41**, 95–98.
- Hebert, P. D., Cywinska, A., Ball, S. L., and deWaard, J. R. (2003). Biological identifications through DNA barcodes. *Proceedings of the Royal Society Biology Sciences* **270**, 1523. doi:10.1098/rspb.2002.2218
- Kimura, M. (1980). A simple method for estimating evolutionary rates of base substitutions through comparative studies of nucleotide sequences. *Journal of Molecular Evolution* **16**, 111–120. doi:10.1007/BF01731581
- Lang, A. S., Bocksberger, G., and Stech, M. (2015). Phylogeny and species delimitations in European *Dicranum* (Dicranaceae, Bryophyta) inferred

- from nuclear and plastid DNA. *Molecular Phylogenetics and Evolution* **92**, 217–225. doi:10.1016/j.ympev.2015.06.019
- Lázaro, E. M., Sluys, R., Pala, M., Stocchino, G. A., Baguña, J., and Riutort, M. (2009). Molecular barcoding and phylogeography of sexual and asexual freshwater planarians of the genus *Dugesia* in the Western Mediterranean (Platyhelminthes, Tricladida, Dugesiidae). *Molecular Phylogenetics and Evolution* **52**, 835–845. doi:10.1016/j.ympev.2009.04.022
- Leal-Zanchet, A. M., Rossi, I., Seitenfus, A. L. R., and Alvarenga, J. (2012). Two new species of land flatworms and comments on the genus *Pasipha* Ogren & Kawakatsu, 1990 (Platyhelminthes: Continenticola). *Zootaxa* **3583**, 1–21.
- Leliaert, F., Verbruggen, H., Wysor, B., and De Clerck, O. (2009). DNA taxonomy in morphologically plastic taxa: algorithmic species delimitation in the *Boodlea* complex (Chlorophyta: Cladophorales). *Molecular Phylogenetics and Evolution* **53**, 122–133. doi:10.1016/j.ympev.2009.06.004
- Marcus, E. (1951). *Turbellaria brasileiros* (9). *Boletim da Faculdade de Filosofia, Ciências e Letras da Universidade de São Paulo. Série Zoologia* **16**, 1–217.
- Monaghan, M. T., Wild, R., Elliot, M., Fujisawa, T., Balke, M., Inward, D. J. G., and Vogler, A. P. (2009). Accelerated species inventory on Madagascar using coalescent-based models of species Delineation. *Systematic Biology* **58**(3), 298–311. doi:10.1093/sysbio/syp027
- Negrete, L., and Brusa, F. (2016). Land flatworms of the genus *Pasipha* (Platyhelminthes, Geoplanidae) in Argentina, with description of three new species. *Zootaxa* **4137**(2), 187–210. doi:10.11646/zootaxa.4137.2.2
- Puillandre, N., Koua, D., Favreau, P., Oliveira, B. M., and Stöcklin, R. (2012). Molecular phylogeny, classification and evolution of conopeptides. *Journal of Molecular Evolution* **74**, 297–309. doi:10.1007/s00239-012-9507-2
- Ronquist, F., Teslenko, M., van der Mark, P., Ayres, D. L., Darling, A., Höhna, S., Larget, B., Liu, L., Suchard, M. A., and Huelsenbeck, J. P. (2012). MrBayes 3.2: efficient Bayesian phylogenetic inference and model choice across a large model space. *Systematic Biology* **61**, 539–542. doi:10.1093/sysbio/sys029
- Rossi, I., Amaral, S. V., Ribeiro, G. G., Cauduro, G. P., Fick, I., Valiati, V. H., and Leal-Zanchet, A. M. (2015). Two new Geoplaninae species (Platyhelminthes: Continenticola) from Southern Brazil based on an integrative taxonomic approach. *Journal of Natural History* **50**, 1–29. doi:10.1080/00222933.2015.1084057
- Saez, A. G., and Lozano, E. (2005). Body doubles. *Nature* **433**, 111. doi:10.1038/433111a
- Seitenfus, A. L. R., and Leal-Zanchet, A. M. (2004). Uma introdução à morfologia e taxonomia de planárias terrestres (Platyhelminthes, Tricladida, Terricola). *Acta Biologica Leopoldensia* **26**(2), 187–202.
- Sluys, R., Mateos, E., Riutort, M., and Álvarez-Presas, M. (2016). Towards a comprehensive, integrative analysis of the diversity of European microplanid land flatworms (Platyhelminthes, Tricladida, Microplaninae), with the description of two peculiar new species. *Systematics and Biodiversity* **14**, 9–31. doi:10.1080/14772000.2015.1103323
- Stamatakis, A. (2006). RAxML-VI-HPC: maximum likelihood-based phylogenetic analyses with thousands of taxa and mixed models. *Bioinformatics* **22**(21), 2688–2690. doi:10.1093/bioinformatics/btl446
- Swofford, D. L. (2002). 'PAUP\*. Phylogenetic Analysis Using Parsimony (\*and other methods). Version 4.0b10.' (Sinauer Associates: Sunderland, MA, USA.)
- Talavera, G., Dinca, V., and Vila, R. (2013). Factors affecting species delimitations with the GMYC model: insights from a butterfly survey. *Methods in Ecology and Evolution* **4**, 1101–1110. doi:10.1111/2041-210X.12107
- Tamura, K., Stecher, G., Peterson, D., Filipski, A., and Kumar, S. (2013). MEGA6: Molecular Evolutionary Genetics Analysis Version 6.0. *Molecular Biology and Evolution* **30**, 2725–2729. doi:10.1093/molbev/mst197
- Vieites, D. R., Wollenberg, K. C., Andreone, F., Kohler, J., Glaw, F., and Vences, M. (2009). Vast underestimation of Madagascar's biodiversity evidenced by an integrative amphibian inventory. *Proceedings of the National Academy of Sciences of the United States of America* **106**, 8267–8272. doi:10.1073/pnas.0810821106
- Winsor, L. (1998). Aspects of taxonomy and functional histology in terrestrial flatworms (Tricladida: Terricola). *Pedobiologia* **42**, 412–432.
- Zhang, J. J., Kapli, P., Pavlidis, P., and Stamatakis, A. (2013). A general species delimitation method with applications to phylogenetic placements. *Bioinformatics* **29**(22), 2869–2876. doi:10.1093/bioinformatics/btt499

Handling editor: Nerida Wilson